

Toward More Precise Radiotherapy Treatment of Lung Tumors

S.S. Iyengar, *Florida International University*

Xin Li, Huanhuan Xu, and Supratik Mukhopadhyay, *Louisiana State University*

N. Balakrishnan, *Indian Institute of Science*

Amit Sawant and Puneeth Iyengar, *University of Texas Southwestern Medical Center*

A computational framework for modeling the respiratory motion of lung tumors provides a 4D parametric representation that tracks, analyzes, and models movement to provide more accurate guidance in the planning and delivery of lung tumor radiotherapy.

Lung cancer is the most common cause of cancer-related deaths in the US, with only 10 to 15 percent of lung cancer patients surviving five years after diagnosis.¹ More than half of all solid tumors receive external beam ionizing radiation as part of treatment that combines radiotherapy with chemotherapy or with surgery and chemotherapy. The ultimate goal of radiation treatment, or radiotherapy, is to treat the disease while avoiding damage to the normal tissue and critical organs that surround the tumor.

Much research is directed to lung cancer radiotherapy, yet there is room for significant improvement. Conventional radiotherapy involves administering a prescribed tumor-killing dose, typically around 50 to 70 Gray (Gy: a unit of absorbed radiation dose) over anywhere from 25 to 35 sessions, or treatment fractions.

Technological advances and a deeper understanding of radiobiology—the study of how human tissue responds to high doses of x-ray radiation therapy—have enabled two alternatives. The first is to deliver the same total dose in significantly fewer fractions, say one to five, and accom-

pany delivery with improved image guidance using offline and online projection x-ray imaging and computed tomography (CT). The second is to increase the total radiation dose using the historical dose per fraction (2 Gy) with the same image guidance. Literature on lung tumor irradiation has frequently cited the benefits to local tumor control of escalating the dose per fraction.²

The spatial relationship of lung tumors with important normal tissue structures, such as the spinal cord, esophagus, heart, brachial plexus, normal lung tissue, bronchial tree, and trachea, make total dose escalation infeasible in many cases. Moreover, the motion of tumors during respiration complicates radiation treatment planning for lung cancer. The respiratory cycle also involves movement of normal tissue structures. This movement heavily influences tumor motion, which in turn affects the tumor's shape, resulting in the deformation of both the tumor and surrounding organs. For these reasons, treatment planning for intrathoracic radiation (radiation within the chest cavity) requires tools that can provide the highest delivery precision and accuracy.



Figure 1. A patient being treated with external beam radiotherapy using a Varian linear accelerator. Accuracy is essential in lung cancer treatment because respiratory movements can cause the tumor and its surrounding tissue to move and change shape.

To meet that need, we propose a lung tumor modeling and computational framework that facilitates the tracking and prediction of respiratory movement and the deformation of organs surrounding the tumor. Preliminary results of our framework’s application show that, relative to ex-

isting methods, it is more accurate and computationally efficient in the radiotherapy treatment of lung cancer. It is also flexible enough to generalize to the radiotherapy treatment of other pathologies.

RADIOTHERAPY’S CHALLENGES

Radiotherapy treatment typically begins with the patient entering the radiation treatment room and lying supine on the treatment table, as in Figure 1. For lung radiotherapy treatment, the patient is generally in a customized immobilization device to limit natural motion during treatment. In-room lasers ensure that the patient is in the right 3D position with respect to the radiation treatment machine.

Outside the treatment room, physicians and staff take mega- and kilovolt images of the patient to make sure that the subsequent radiation will adequately treat the tumor. Finally, the radiotherapist initiates the radiation treatment, carefully monitoring the patient during the process.

Studies have amassed considerable scientific evidence on both the benefits of dose escalation and the perils of normal tissue toxicity, and there have been tremendous gains in radiotherapy planning and delivery precision. These developments have made it critical for radiotherapy treatment to accurately capture the geometry of the temporarily deforming organ, particularly in lung cancer radiotherapy, in which respiratory motion causes thoracic anatomy to change continuously in all four dimensions—3D space and time.

The ideal radiotherapy guidance requires complete spatiotemporal knowledge of the movement and deformation of the volume—the region that includes the solid tumor and

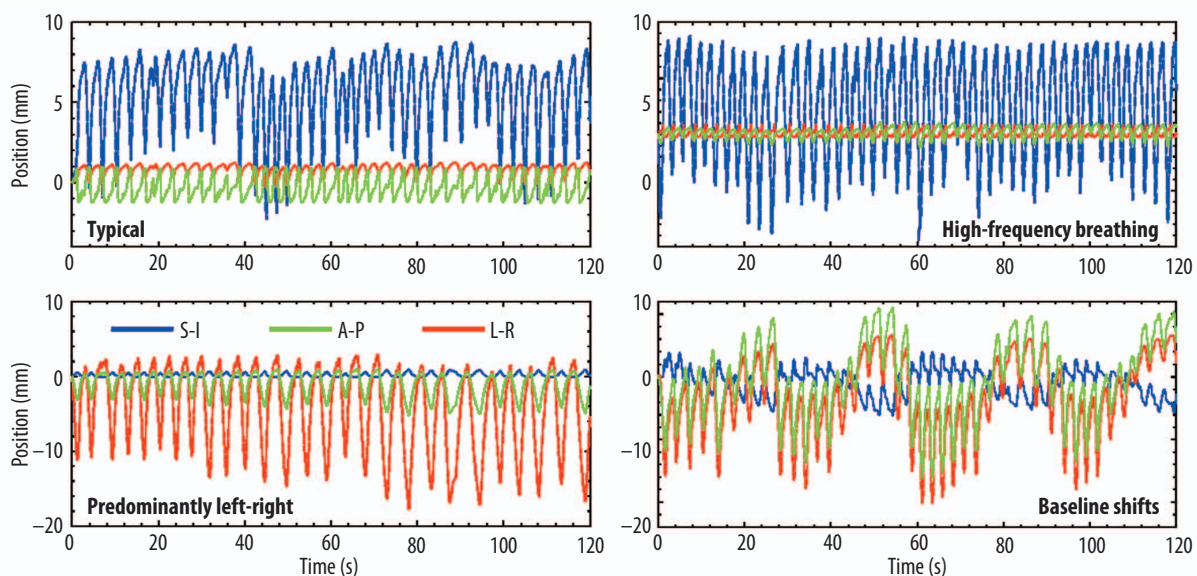


Figure 2. Representative lung tumor motion traces recorded from four patients using the Synchrony system. The traces are indicative of the wide variety of respiratory patterns that are observed clinically. (Image from Y. Suh et al., “An Analysis of Thoracic and Abdominal Tumor Motion for Stereotactic Body Radiotherapy Patients,” *Physics in Medicine and Biology*, July 2008, pp. 3623-3640.)

surrounding tissues and organs—to be treated. However, pretreatment imaging remains one of the weakest aspects of current radiotherapy guidance. Typically, radiotherapists use 4DCT to acquire raw CT images or projections over several respiratory cycles. An external motion monitor aids in phase or amplitude sorting,³ placing projections into bins according to respiratory phase⁴ or displacement, respectively. Pretreatment imaging ends with the generation of a time series of 3D volumes, which describes the volume's motion over a single representative cycle.

Typically, radiotherapists use a maximum- or average-intensity projection (MIP or AIP) from all phases to define a motion-inclusive internal target volume. The MIP represents the superposition; the AIP is the average. The internal target volume serves as the basis for a treatment plan and becomes the ground truth for subsequent radiotherapy stages.

Although researchers have proposed various strategies to improve 4DCT-based planning and delivery paradigms, several fundamentally challenging issues remain to be tackled:

One issue is cycle-to-cycle complexities. As Figure 2 shows, respiratory motion is more complex than a single cycle can characterize. MIP and AIP images do not account for these complexities, which can lead to errors.⁵ Another challenge stems from forcing CT projection data from several cycles into a few respiratory phase bins, which can lead to severe artifacts. Figure 3 shows some examples of these severities. Indeed, one study found that 45 of 50 patients had at least one artifact, ranging in size from 4.4 to 56.0 mm (mean magnitude of 11.6 mm).⁶

Finally, at 29 to 40 milliSieverts (mSv; Sievert is the unit of any of the quantities expressed as dose equivalent), the equivalent dose for 4DCT is about four times higher than that for 3DCT (3 to 10 mSv).⁷ Such a high imaging dose discourages more frequent imaging and long-term monitoring.

These challenges make it highly desirable to have a computational radiotherapy-guidance strategy that uses a 4D motion model developed from 4D magnetic resonance imaging (MRI) and a planning 3DCT acquired at a reference phase. The idea is to update the model with real-time position information and then deliver the corresponding updated radiation fluence map (a 2D map of the x-ray intensity distribution from the medical linear accelerator).

COMPUTATIONAL FRAMEWORK

To accurately model the tumor and surrounding sensitive structures, we developed a 4DCT geometric modeling framework⁸ that tackles several important tasks in analyzing and processing 3DCT volumes and sequential fluoroscopy images (projected 2D images). Our current framework uses temporally dense MR images (sliced 2D images) to refine our integrated 3DCT volumes. Registering MR images with 3D volumes is usually simpler and can be more robust.

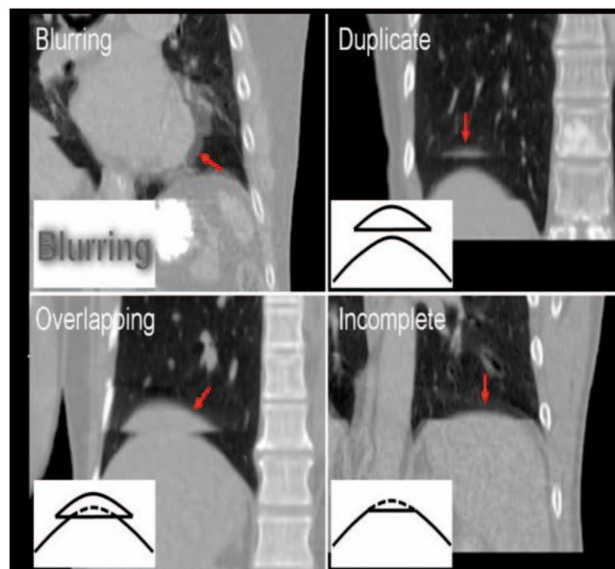


Figure 3. Examples of motion-induced artifacts observed in lung 4DCT. Clockwise from top left: blurring, duplicate, incomplete, and overlapping artifacts. (Image from T. Yamamoto et al., "Retrospective Analysis of Artifacts in Four-dimensional CT Images of 50 Abdominal and Thoracic Radiotherapy Patients," *Int'l J. Radiation Oncology, Biology, and Physiology*, vol. 72, no. 4, 2008, pp. 1250-1258.)

A 4D model parameterizes irradiation volume temporally. From this deforming 4D parametric model, it is possible to extract a tight planning margin to spare normal tissues from dose radiation during delivery.

As Figure 4 shows, our framework has two phases: offline modeling and planning, and online prediction and delivery. As their names imply, the first phase focuses on modeling tumor motion and planning radiotherapy, while the second phase helps guide treatment delivery.

Offline modeling and planning

The offline phase is concerned with modeling the tumor's motion and deformation. To better predict tumor movement, which could be affected by neighboring organs and tissues during respiration, the model covers the entire neighboring volume region.

Contour segmentation. The first step in this phase is to clearly segment the tumor and surrounding structures within the potential irradiated volume from 3DCT or MR images. Because reliable 3D image segmentation against noise is critical at this stage, we developed the template-guided graph cut (TGGC) algorithm.

To perform the 3D graph cut, the algorithm uses a novel metric that combines image intensity (noise filtered) and a predesigned implicit scalar field that captures the template shape and serves as a reference. TGGC reaches globally optimal segmentation; simple user interactions can iteratively

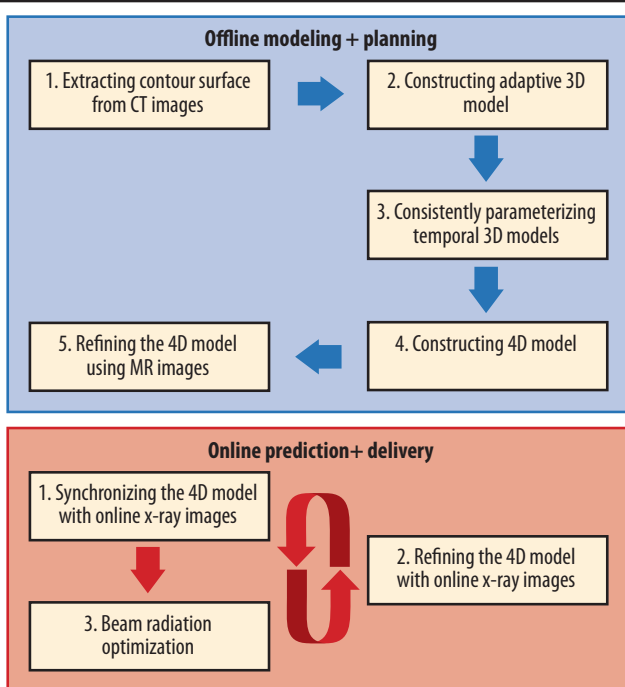


Figure 4. Two phases in the computational framework. The first phase, offline modeling and planning, emphasizes radiotherapy planning and is based on CT and magnetic resonance (MR) scans. The second phase focuses on online prediction and treatment delivery. Real-time scanned 2D images aid in synchronizing and refining the 4D model, which the system uses to predict the tumor's trajectory and geometry and guide treatment delivery.

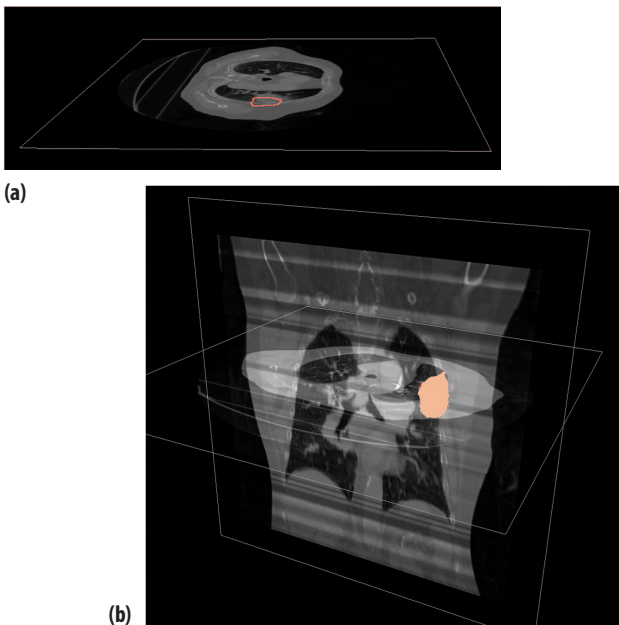


Figure 5. Tumor segmentation from CT images. (a) Segmentation performed in 3D; the red solid is the tumor; (b) segmentation visualized in a cross-section.

and adaptively refine the extracted contour. A postprocess uses morphological operations (performing open then close operations with radius-3 disks) to smooth the extracted contour.

Figures 5 and 6 show our preliminary results. Figures 6a through 6d show that TGGC is superior to existing segmentation methods in extracting the object of interest from the image background. Figures 6a through 6c show the results of using the level set,⁹ watershed,¹⁰ and original graph cut¹¹ methods, respectively. Compared with the level set method, a popular method of segmenting medical image data, TGGC takes about a third of the computation time to segment the entire 3DCT volume. The segmentation also more tightly bounds the tumor's contour. Although faster than TGGC, the watershed method leads to significant oversegmentation, an outcome that TGGC avoids.

From volume image to a tetrahedral mesh. After extracting contours of both the tumor and surrounding structures, our framework models both the geometry and material of the entire volume instead of modeling only boundary shells. It then adaptively tetrahedralizes (converts a volume image into a tetrahedral mesh) the irradiated volume.

Figure 7 illustrates an example of a tetrahedral representation of a tumor and surrounding tissue. Such a finite element representation is much sparser than the grid-based image representation, and any local region can be coarsened or refined adaptively when necessary. This effectively represents the region's inherent structure, while conforming to important features and materials. It is then possible to use a linear interpolation or a spline function to represent the deforming irradiated volume.

One critical issue is how to compute the optimal sampling points for tetrahedralization. Given the number of sample points, the goal is to minimize the mean square error (mean of the square difference) between the linear interpolation and the corresponding original intensity values. Intuitively, selected points should balance the uniformity and the sampling of sharp features. It is then possible to use Delaunay tetrahedralization to tessellate the model on these sampled points.

Volumetric mapping and interpolation. After representing volumetric regions of interest using tetrahedral meshes, our algorithm computes bijective volumetric mapping to consistently parameterize 3D volumes and then interpolate the 4D temporal model.

Bijective volumetric mapping involves computing a lowly distorted mapping (small angle and area distortion, which is physically natural) between two consecutive volumes through a coarse-to-fine framework. Initially, the algorithm extracts corresponding features and matches them in 3D. Then taking these features as soft constraints, it computes surface and volumetric mappings¹² between corresponding contours and volumes. The result is a consistent

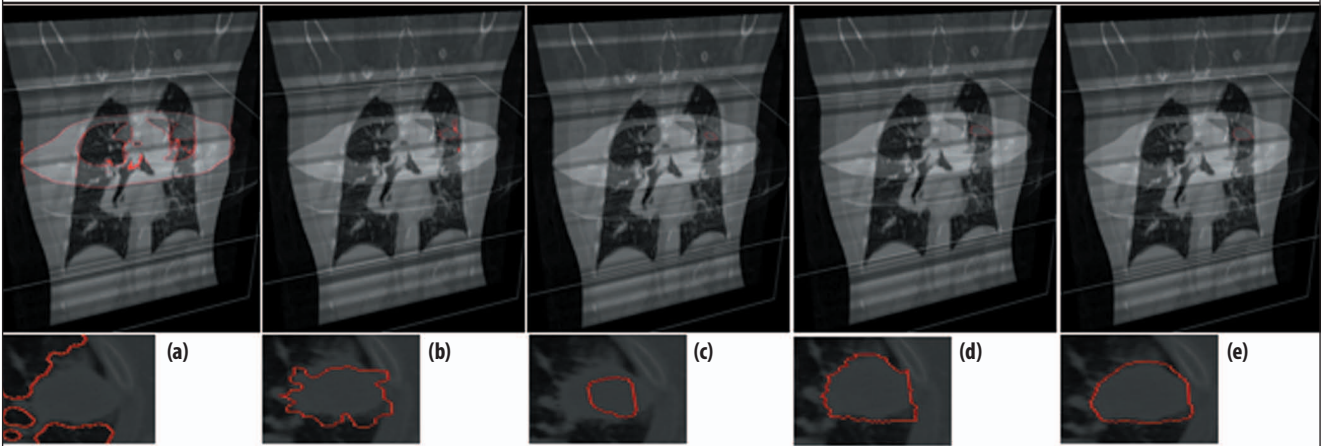


Figure 6. Comparison of segmentation results. Tumor contour segmentation based on (a) level set method, (b) watershed method, (c) original graph cut method, and our TGGC algorithm (d) without de-noise and (e) with de-noise. The final segmentation (e) is suitable for subsequent tumor modeling and tracking tasks.

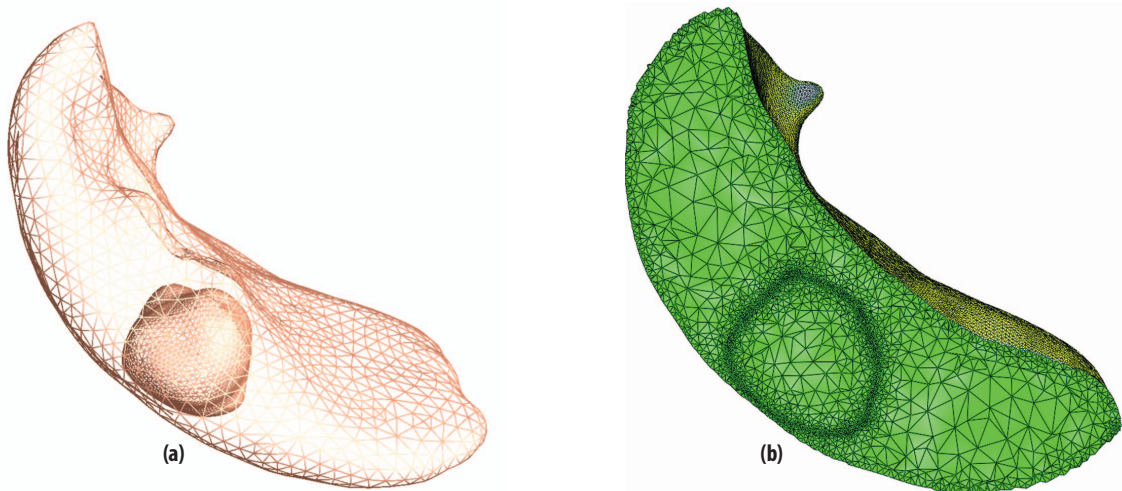


Figure 7. Tumor and surrounding lobe: (a) contour surfaces and (b) adaptive conversion to a tetrahedral mesh.

parameterization of all temporally sequential volumes onto one common domain $D(u,v,w)$.

With this one-to-one correspondence in hand, the algorithm can create a continuously deforming 4D model— $M(u,v,w,t)$ —by computing the physically natural shape interpolation between two consequent models. Given the (u,v,w) parameter coordinate in the domain, it can trace a point's trajectory under different time t ; similarly, given any t , it can obtain the 3D volume's location and geometry at that moment.

4D model refinement. The first three steps in this phase rely on CT images, which can have very high resolution and thus very good spatial accuracy. However, CT imaging requires a high dose, and a frequent and long CT imaging sequence is impossible. For this reason, CT-sampled volumes tend to be temporally sparse.

To compensate for this disadvantage, our algorithm refines the 4D model computed in the previous mapping

and interpolation step using a sequence of 3D MR images and cross-model volumetric parameterization to register the volume from the MRI and the interpolated volume. It can then correct the consistently deforming 4D model according to the matching results. The refined continuous parametric 4D model is ready for use in determining the trajectory and geometry of the volume of interest.

Refining the 4D model and predicting motion

In the online phase, our framework uses real-time scanned 2D images (orthogonally mounted x-ray) to synchronize and refine the 4D model. From the refined 4D model, the framework can then predict the tumor's trajectory and geometry. This prediction makes it easier to optimize the treatment beam to target the most desirable radiation positions.

Model synchronization and refinement. During radiation delivery, it is possible to obtain a 2D time series

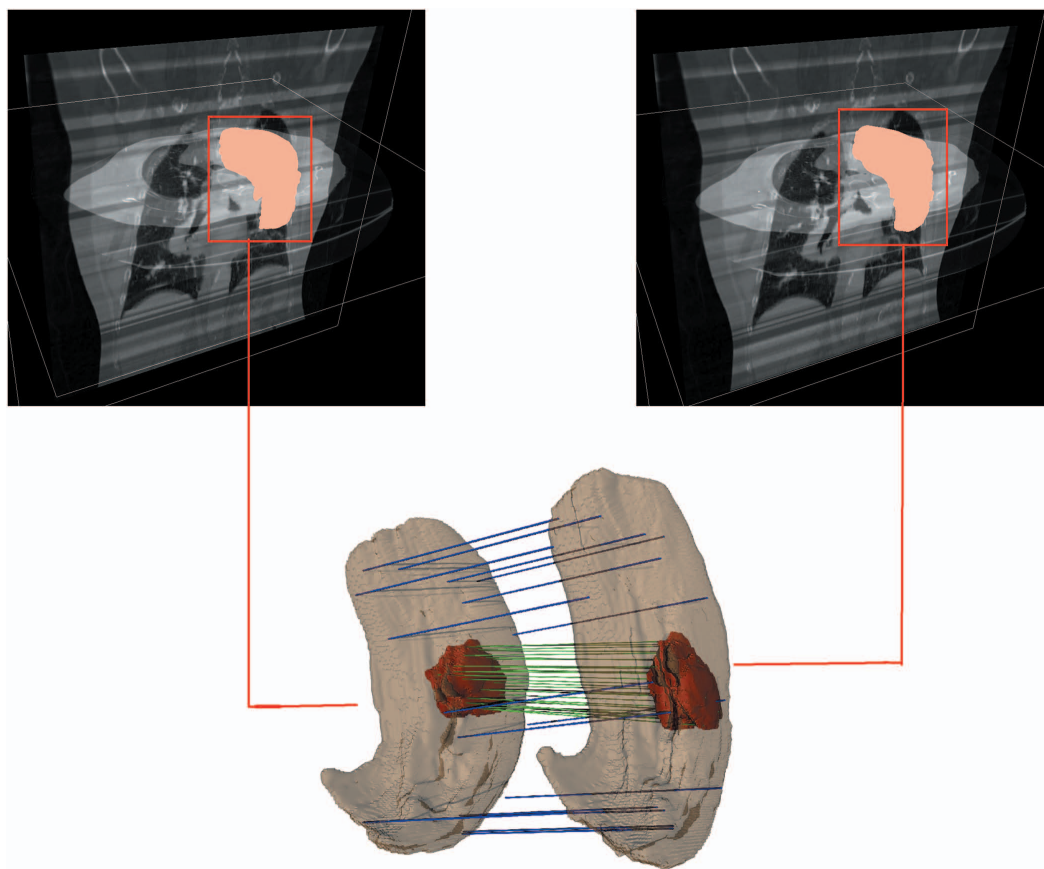


Figure 8. Tracking temporally deforming tumor and surrounding lobe. The red area represents the tumor under two time sequences. Green and blue lines indicate the correspondence between the solid regions in the two time frames (the 3D tumor and lobe at the bottom row are rotated 90 degrees in the y -axis to better visualize the matching).

of x-ray projection images and register them with the moving 3D model. Our framework then uses the results of the matching to correct the 4D model. The optimal mapping is searchable within a conservative time range, starting from the last synchronized point.

Beam radiation optimization. With the deforming 3D volume, it is possible to optimize the beam's radiation direction. As Figure 8 shows, ideally, the beam should be planned so that it can see the tumor clearly without being visually blocked by other organs. Otherwise, the radiation will hit those organs before it reaches the tumor. To solve this problem, we propose using an efficient hierarchical integer linear program (HILP). Our recent work in autonomous robotic environment inspection has demonstrated that an HILP scheme can be very efficient in solving this challenging 3D region-inspection problem.¹³

Our computation framework and platform for lung tumor modeling and tracking can greatly enhance radiotherapy planning and delivery, in large

part because it effectively integrates reliable 3D image segmentation; volumetric modeling, analysis, and parameterization; physical and geometric interpolation; and tracking techniques. Generalizing our computation paradigm would allow other medical planning and treatment regimens to benefit from this integration.

Our framework already cuts segmentation preprocessing time by roughly two-thirds, and we expect advances in parallelism to decrease that time even further. Segmentation preprocessing takes $O(n \log n)$ time and $O(n)$ space, where n is the pixel number of each volume image. We can solve volumetric mapping computation within $O(m^3)$ time and $O(m^2)$ space, where m is the vertex number of interested objects.

All these geometric computation algorithms are local and can be effectively parallelized. Using GPUs can improve the entire pipeline's efficiency. We plan to explore a GPU implementation and expect to achieve significant efficiency improvement in both offline data analysis and planning, and greater optimization of real-time treatment. **□**

Acknowledgments

This project is partially supported by Louisiana Board of Regents Post Katrina Funds, Louisiana Board of Regents Research Competitiveness Subprogram LEQSF(2009-12)-RD-A-06, PFund: NSF(2011)-PFund-236, and LSU Faculty Research Grant 2010.

We thank the anonymous reviewers for their comments and the coordinating editor for valuable assistance in revising an earlier version of this article. We also thank Yang Wang from Siemens Corporate Research for valuable discussions during this project.

References

1. A. Jemal et al., "Cancer Statistics, 2008," *CA: A Cancer J. for Clinicians*, vol. 58, no. 2, 2008, pp. 71-96.
2. A.W. Blackstock and R. Govindan, "Definitive Chemoradiation for the Treatment of Locally Advanced Non-Small-cell Lung Cancer," *J. Clinical Oncology*, vol. 25, no. 26, 2007, pp. 4146-4152.
3. N. Wink, C. Panknin, and T.D. Solberg, "Phase versus Amplitude Sorting of 4D-CT Data," *J. Applied Clinical Medicine and Physiology*, vol. 7, no. 1, 2006, pp. 77-85.
4. G.S. Mageras et al., "Measurement of Lung Tumor Motion Using Respiration-Correlated CT," *Int'l J. Radiation Oncology, Biology, and Physiology*, vol. 60, no. 3, 2004, pp. 933-941.
5. J. Cai et al., "Estimation of Error in Maximal Intensity Projection-Based Internal Target Volume of Lung Tumors: A Simulation and Comparison Study Using Dynamic Magnetic Resonance Imaging," *Int'l J. Radiation Oncology, Biology, and Physiology*, vol. 69, no. 3, 2007, pp. 895-902.
6. T. Yamamoto et al., "Retrospective Analysis of Artifacts in Four-Dimensional CT Images of 50 Abdominal and Thoracic Radiotherapy Patients," *Int'l J. Radiation Oncology, Biology, and Physiology*, vol. 72, no. 4, 2008, pp. 1250-1258.
7. S. Mori et al., "Effective Doses in Four-Dimensional Computed Tomography for Lung Radiotherapy Planning," *Medical Dosimetry*, vol. 34, no. 1, 2008, pp. 87-90.
8. Y. Miyabe et al., "New Algorithm to Simulate Organ Movement and Deformation for Four-Dimensional Dose Calculation Based on a Three-Dimensional CT and Fluoroscopy of the Thorax," *Medical Physics*, vol. 36, no. 10, 2009, pp. 4328-4339.
9. T.F. Chan and L.A. Vese, "Active Contours without Edges," *IEEE Trans. Image Processing*, vol. 10, no. 2, 2001, pp. 266-277.
10. F. Meyer, "Topographic Distance and Watershed Lines," *Signal Processing*, vol. 38, no. 1, 1994, 2001, pp. 113-125.
11. Y. Boykov and G. Funka-Lea, "Graph Cuts and Efficient N-D Image Segmentation," *Int'l J. Computer Vision*, Nov. 2006, pp. 109-131.
12. X. Li et al., "Meshless Harmonic Volumetric Mapping Using Fundamental Solution Methods," *IEEE Trans. Automation Science Eng.*, vol. 6, no. 3, 2009, pp. 409-422.
13. X. Li et al., "On Optimizing Autonomous Pipeline Inspection," *IEEE Trans. Robotics*, Nov. 2011, pp. 1-11.

S.S. Iyengar is a professor of computer science and the director of the School of Computing Science and Information Computing at Florida International University. His research interests in-

clude the design and analysis of high-performance algorithms, image analysis for medical applications, distributed sensor networks, parallel and distributed computing, and computational aspects of robotics applications. Iyengar received a PhD in general engineering from Mississippi State University. He is a Fellow of IEEE, ACM, and the American Association for the Advancement of Science and a member of the European Academy of Sciences. Contact him at iyengar@cs.fiu.edu.

Xin Li is an assistant professor in the Department of Electrical and Computer Engineering and in the Center for Computational and Technology at Louisiana State University. His research interests include geometric modeling, computer graphics, vision, and visualization. Li received a PhD in computer science from Stony Brook University. He is a member of the IEEE Computer Society and ACM. Contact him at xinli@cct.lsu.edu or www.ece.lsu.edu/xinli.

Huanhuan Xu is a PhD candidate in the Department of Electrical and Computer Engineering at Louisiana State University. Her research interests include geometric modeling and image processing. Xu received an MSc in computer science from the University of Science Technology of China. Contact her at huanxu4@cct.lsu.edu.

Supratik Mukhopadhyay is an assistant professor in the Department of Computer Science at Louisiana State University. His research interests include video analytics, inference, software engineering, and programming languages. Mukhopadhyay received a PhD in program verification from the Max Planck Institute for Computer Science. Contact him at supratik@csc.lsu.edu.

N. Balakrishnan is the associate director of the Indian Institute of Science (IISc), Bangalore. His research interests include high-performance computing, information security, and computational electromagnetics. Balakrishnan received a PhD in engineering from IISc. Contact him at balki@serc.iisc.ernet.in.

Amit Sawant is an assistant professor in the Department of Radiation Oncology at the University of Texas Southwestern Medical Center, Dallas. His research interests include real-time motion management and image guidance for thoracic and abdominal radiation therapy. Sawant received a PhD in biomedical engineering from the University of Michigan. Contact him at amit.sawant@utsouthwestern.edu.

Puneeth Iyengar is the Ryder Professor and director of the Department of Radiation Oncology at the University of Texas Southwestern Medical Center. He treats lung cancer patients and has a laboratory that focuses on elucidating the complex interactions that occur in the setting of inflammatory-driven malignancies. Iyengar received an MD and a PhD in cell biology from the Albert Einstein College of Medicine. Contact him at puneeth.iyengar@utsouthwestern.edu.



Selected CS articles and columns are available for free at <http://ComputingNow.computer.org>.